Supporting Information

de Boer et al. 10.1073/pnas.1100555108

SI Text

The biochemical model of photosynthesis (1) requires three species-specific photosynthesis parameters (at 25 °C) to be known: maximum carboxylation capacity [V_{cmax25} ($mol \cdot m^{-2} \cdot s^{-1}$)], maximum rate of electron transport [J_{max25} ($mol \cdot m^{-2} \cdot s^{-1}$)] and mitochondrial respiration rate R_{d25} ($mol \cdot m^{-2} \cdot s^{-1}$) (Table S2). For *Pinus taeda* (Pt) and *Taxodium distichum* (Td), we derived these values from published A/C_i curves (2) and the empirical relation among V_{cmax25}, J_{max25}, and R_{d25} (3, 4):

$$J_{max25} = \left(29.1 + 1.64 \cdot 10^6 \cdot V_{cmax25}\right) \cdot 10^{-6} \qquad \textbf{[S1]}$$

and

$$R_{d25} = 0.015 \cdot V_{cmax25}. \qquad \textbf{[S2]}$$

For the other species [*Acer rubrum* (Ar), *Ilex cassine* (Ic), *Myrica cerifera* (Mc), *Quercus laurifolia* (Ql), *Quercus nigra* (Qn), *Pinus elliottii* (Pe), and *Pinus taeda* (Pt)], we derived V_{cmax25} and J_{max25} from foliar nitrogen content (5) and R_{d25} from Eq. **S2**:

$$V_{cmax25} = 6.25 \cdot V_{cr} M_A N_m P_R \cdot 10^{-6}, \qquad \textbf{[S3]}$$

where 6.25 is the ratio of weight of Rubisco to the weight of nitrogen in Rubisco ($g \cdot g^{-1}$), V_{cr} is the specific activity of Rubisco at 25 °C [20.7 ($\mu mol \cdot g^{-1} \cdot s^{-1}$)], M_A is the leaf mass ($g \cdot m^{-2}$), N_m is leaf nitrogen content per leaf dry mass ($g \cdot g^{-1}$) and P_R (-) is the fraction of nitrogen allocated to Rubisco, estimated at 0.15, and:

$$J_{max25} = 8.06 \cdot J_{mc} M_A N_m P_B \cdot 10^{-6}, \qquad \textbf{[S4]}$$

where 8.06 is the minimal nitrogen investment in cytochrome bioenergetics [μmol of cytochrome·(g of N)$^{-1}$], the potential rate of photosynthetic electron transport per unit cytochrome (J_{MC}) is estimated at 156 μmol electrons·(μmol of cytochrome·s)$^{-1}$ at 25 °C and PB (g of N in cytochrome) is the fraction of N allocated to RuBP estimated at 0.035.

Down-regulation of the photosynthesis parameters V_{cmax25} and J_{max25} in response to rising CO_2 (6, 7) is simulated with an exponential decay function:

$$V_{cmax25}\left(CO_2\right) = V_{cmax25}\left(385\right) \cdot e^{-\kappa(CO_2 - 385)} \qquad \textbf{[S5]}$$

and

$$J_{max25}\left(CO_2\right) = J_{max25}\left(385\right) \cdot e^{-\kappa(CO_2 - 385)}, \qquad \textbf{[S6]}$$

where $V_{cmax25}(385)$ and $J_{max25}(385)$ represent the photosynthesis parameters V_{cmax25} and J_{max25} at their present day values (Table S2) and κ is a decay constant for the CO_2 response of V_{cmax25} and $J_{max25.}$ A value of $2 \cdot 10^{-4}$ ppm^{-1} is chosen for κ to match estimated down-regulation of photosynthesis parameters at geological timescales (7). Furthermore, species specific values of leaf area index [LAI (-)] are derived from literature (Table S2) (8, 9).

1. Farquhar GD, von Caemmerer S, Berry JA (2001) Models of photosynthesis. *Plant Physiol* 125:42–45.
2. Ellsworth DS, et al. (2004) Photosynthesis, carboxylation and leaf nitrogen responses of 16 species to elevated pCO2 across four free-air CO2 enrichment experiments in forest, grassland and desert. *Glob Change Biol* 10:2121–2138.
3. Wullschleger SD (1993) Biochemical limitations to carbon assimilation in C3 plants–a retrospective analysis of the A/Cl curves from 109 species. *J Exp Bot* 44:907–920.
4. Baldocchi DD, Wilson KB (2001) Modeling CO2 and water vapor exchange of a temperate broadleaved forest across hourly to decadal time scales. *Ecol Modell* 142:155–184.
5. Niinemets Ü, Tenhunen JD (1997) A model separating leaf structural and physiological effects on carbon gain along light gradients for the shade-tolerant species Acer saccharum. *Plant Cell Environ* 20:845–866.
6. Ainsworth EA, Rogers A (2007) The response of photosynthesis and stomatal conductance to rising [CO2]: Mechanisms and environmental interactions. *Plant Cell Environ* 30:258–270.
7. Franks PJ, Beerling DJ (2009) CO(2)-forced evolution of plant gas exchange capacity and water-use efficiency over the Phanerozoic. *Geobiology* 7:227–236.
8. Vose JM, et al. (1995) Vertical leaf area distribution, light transmittance, and application of the Beer-Lambert Law in four mature hardwood stands in the southern Appalachians. *Can J For Res* 25:1036–1043.
9. Liu S, Riekerk H, Gholz H (1997) Leaf litterfall, leaf area index, and radiation transmittance in cypress wetlands and slash pine plantations in north-central Florida. *Wetlands Ecol Manage* 4:257–271.
10. Clark KL, Gholz HL, Castro MS (2004) Carbon dynamics along a chronosequence of slash pine plantations in North Florida. *Ecological Applications* 14:1154–1171.
11. Powell TL, et al. (2008) Carbon exchange of a mature, naturally regenerated pine forest in north Florida. *Glob Change Biol* 14:2523–2538.
12. Franks PJ, Beerling DJ (2009) Maximum leaf conductance driven by CO2 effects on stomatal size and density over geologic time. *Proc Natl Acad Sci USA* 106:10343–10347.
13. Williams M, et al. (1996) Modelling the soil-plant-atmosphere continuum in a Quercus & Acer stand at Harvard Forest: The regulation of stomatal conductance by light, nitrogen and soil/plant hydraulic properties. *Plant Cell Environ* 19:911–927.
14. Saha AK, Sternberg LDSLO, Miralles-Wilhelm F (2009) Linking water sources with foliar nutrient status in upland plant communities in the Everglades National Park, USA. *Ecohydrology* 2:42–54.
15. Moorhead KK, McArthur J (1996) Spatial and temporal patterns of nutrient concentrations in foliage of riparian species. *Am Midl Nat* 136:29–41.

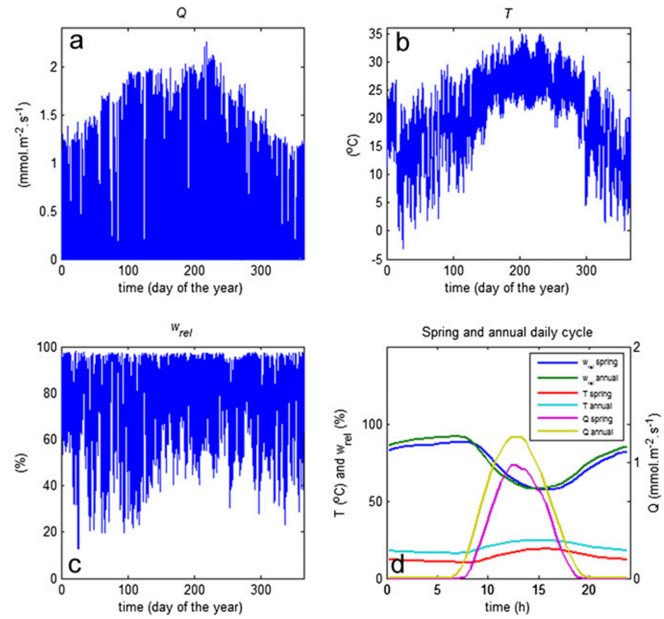

Fig. S1. Environmental boundary conditions used to force stomatal adaptation models. Annual cycles of climatic boundary conditions of photosynthetic active radiation [Q (mmol·m^{-2}·s^{-1})] (*A*), ambient air temperature [T (°C)] (*B*), and relative humidity [w_{rel} (%)] (*C*) measured over a pine flatwoods ecosystem near Gainesville, FL, during the year 2003 (10, 11). (*D*) Average diurnal cycles for Q, T, and w_{rel} during leaf development (March, April, and May) are prescribed to the optimization model to determine g_{smax}. Annual average diurnal cycles of these boundary conditions are prescribed to calculate gas exchange at the leaf level. A complete annual cycle of these boundary conditions is prescribed to calculate changes in annual canopy transpiration.

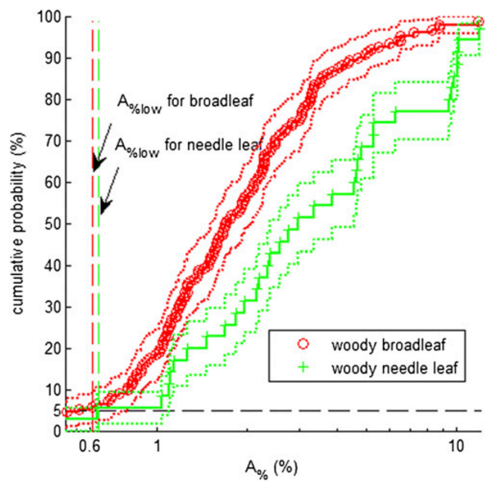

Fig. S2. Empirical cumulative probability of $A_{\%}$ for woody broadleaf and woody needle leaf species. Data are from Franks and Beerling (12). Red circles and green crosses denote data points; dotted red and green lines denote the fit of the empirical distribution together with their 95% confidence levels. Dashed red and green lines denote the lower 5% limit of $A_{\%}$. On average, stomata occupy less space on leaves of woody broadleaf species than on leaves (needles) of woody needle leaf species. However, the 5% lower limit of $A_{\%}$ (defined as $A_{\%\mathrm{low}}$) for both distributions cannot be distinguished. Note that a logarithmic *x* axis is used.

Table S1. Species specific relations between pore length and guard cell width

Species	Mean C_w, μm	σ, μm	*n*	Linear regression	r^2
Acer rubrum	6.79	0.94	36	$C_w = 0.36 \cdot L + 2.90$	0.49*
Ilex cassine	10.26	1.33	27	$C_w = 0.28 \cdot L + 6.19$	0.57*
Myrica cerifera	7.84	1.10	25	$C_w = 0.41 \cdot L + 3.57$	0.62*
Pinus elliottii	16.24	2.22	28	$C_w = 0.27 \cdot L + 6.66$	0.62*
Pinus taeda	11.51	1.22	33	$C_w = 11.5$ μm	—
Quercus laurifolia	6.72	0.77	22	$C_w = 0.27 \cdot L + 4.57$	0.49*
Quercus nigra	7.29	1.21	27	$C_w = 0.26 \cdot L + 3.55$	0.56*
Taxodium distichum	9.79	1.57	20	$C_w = 0.55 \cdot L + 1.52$	0.72*

Species specific relations between pore length (L) and guard cell width (C_w) are used to derive pore depth (l), based on the assumption that l is equal to C_w (1). The SD (σ) and number of measurements (n) are indicated, alongside the linear regressions and r^2 values. Species specific regressions between C_w and L are highly significant ($P < 0.0001$, indicated by *) with exception of *P. taeda*. We therefore derive l from these species specific regressions, except for *P. taeda* for which a constant value is applied. The average slope of these regressions is used to calculate lines of equal g_{smax} in Fig. 1*A*.

Table S2. Species-specific model parameters

Species	λ	LAI	V_{cmax25}	J_{max25}	R_{d25}	Derived from	M_a	Ref.
Acer rubrum	72	5.5	75.0	94	1.1	Foliar N	—	13
Ilex cassine	134	5.5	55.5	79.2	0.8	Foliar N	127 (15)	14
Myrica cerifera	99	5.5	62.5	89.1	0.9	Foliar N	101 (35)	14
Pinus elliottii	244	2	60.9	86.9	0.9	Foliar N	—	14
Pinus taeda	87	2	47.0	77.1	0.7	A/C_i curves	—	2
Quercus laurifolia	62	5.5	54.0	77.0	0.8	Foliar N	102 (34)	15
Quercus nigra	58	5.5	64.8	92.4	1.0	Foliar N	96 (10)	15
Taxodium distichum	55	3	30.0	49.2	0.5	A/C_i curves	—	2

Species specific model parameters. Lagrangian multiplier [λ (μmol.mol^{-1})], leaf area index [LAI (-)] and photosynthesis parameters *Vcmax25*, J_{max25} and R_{d25} (μmol·m^{-2}·s^{-1}) and how photosynthesis parameters are derived. If photosynthesis parameters are based on foliar nitrogen (N) concentrations on a leaf mass base, measurements of leaf mass with area [M_a (g·m^{-2})] and their SDs are indicated. LAI values for conifers (8, 9) are doubled in the model to account for their amphistomatic leaves.